

An experimental and theoretical study of the reactions Na+HCl and Na+DCI

John M. C. Plane, B. Rajasekhar, and Libero Bartolotti

Citation: *The Journal of Chemical Physics* **91**, 6177 (1989); doi: 10.1063/1.457436

View online: <http://dx.doi.org/10.1063/1.457436>

View Table of Contents: <http://scitation.aip.org/content/aip/journal/jcp/91/10?ver=pdfcov>

Published by the [AIP Publishing](#)

Articles you may be interested in

[Time-dependent Quantum Wave Packet Study of F+HCl and F+DCI Reactions](#)

Chin. J. Chem. Phys. **20**, 365 (2007); 10.1088/1674-0068/20/04/365-371

[Time-dependent quantum wave packet studies of the F+HCl and F+DCI reactions](#)

J. Chem. Phys. **113**, 10105 (2000); 10.1063/1.1323504

[Experimental and theoretical study of the reaction K+HCl](#)

J. Chem. Phys. **99**, 7696 (1993); 10.1063/1.466215

[Infrared and Raman Studies of Crystalline HCl, DCI, HBr, and DBr](#)

J. Chem. Phys. **44**, 548 (1966); 10.1063/1.1726724

[Pressure Broadening of DCI by HCl and of HCl by DCI. A Comparison of Experimental Results with Anderson's Theory](#)

J. Chem. Phys. **40**, 534 (1964); 10.1063/1.1725150



An experimental and theoretical study of the reactions Na + HCl and Na + DCl

John M. C. Plane and B. Rajasekhar

Rosenstiel School of Marine and Atmospheric Science, University of Miami, Miami, Florida 33149

Libero Bartolotti

Department of Chemistry, University of Miami, Coral Gables, Florida 33124

(Received 14 April 1988; accepted 8 August 1989)

An experimental study is presented of the reactions Na + HCl/DCl from 590 to 820 K. Na atoms were produced in an excess of HCl/DCl and He bath gas, by the pulsed photolysis of NaCl vapor. The metal atom concentration was then monitored by time-resolved laser induced fluorescence of Na atoms at $\lambda = 589$ nm. A fit of the data to the Arrhenius form yields (2σ uncertainty): $k(\text{Na} + \text{HCl}) = (2.1 \pm 0.5) \times 10^{-9} \exp[(-41.8 \pm 1.5 \text{ kJ mol}^{-1})/RT] \text{ cm}^3 \text{ molecule}^{-1} \text{ s}^{-1}$; $k(\text{Na} + \text{DCl}) = (2.2 \pm 1.0) \times 10^{-9} \exp[(-45.5 \pm 3.8 \text{ kJ mol}^{-1})/RT] \text{ cm}^3 \text{ molecule}^{-1} \text{ s}^{-1}$. The large activation energies are shown to be consistent with vibrational excitation of the hydrogen halides greatly enhancing the reaction cross-sections. A pair of *ab initio* potential surfaces for these reactions are then calculated at constant angle cuts through the lowest ${}^2A'$ hypersurface, including a collinear surface and the surface containing the lowest saddle point which is found to occur at a bent configuration with $\theta_{\text{NaClH}} = 54.7^\circ$. Both surfaces exhibit a late reaction barrier. The effect of reactant vibrational excitation is then demonstrated by using quasiclassical trajectories on the collinear surface.

I. INTRODUCTION

The reactions between the alkali metals and the hydrogen halides have played a central role in the development of reaction dynamics since the 1930s.¹ Because they are generally characterized by large reaction cross sections, this set of reactions was later used in pioneering the molecular beam technique in the 1950s.^{2,3} Since then, the reactions have been studied in great detail, including the effects of translational, vibrational, rotational and electronic excitation of the reagents on the reaction dynamics.^{4,5}

Recently, interest has developed in determining the absolute rate coefficients for these types of reactions as a function of temperature.⁶⁻⁸ Such measurements complement studies in molecular beams by providing direct measurements of activation energies and collision factors which, by making the assumption of a Maxwell-Boltzmann distribution of reactant energies, can yield information about the reaction energy barriers and reaction cross sections.^{7,9} Furthermore, absolute rate measurements at high temperature provide the kinetic information which is required to elucidate the complex chemistry of both alkali and halogenated species in flames.¹⁰

This body of experimental work has prompted a number of theoretical investigations into the nature of the potential energy surfaces governing these reactions. In the case of the reaction



a semiempirical potential energy surface (PES) was generated by Shapiro and Zeiri, who concluded that the reaction had a very late barrier and a nearly collinear transition state. The barrier was estimated to be 58.7 kJ mol^{-1} relative to the HCl minimum. More recently, Gallo and Yarkony¹² carried out an *ab initio* study of reaction (1), for which they deter-

mined a bent transition state with $\theta_{\text{NaClH}} = 55.1^\circ$, and a barrier height of 72.3 kJ mol^{-1} (which increased to $100.7 \text{ kJ mol}^{-1}$ when electron correlation was included).

In this paper we will report a study of reaction (1) and the isotopic reaction



in which absolute second-order rate constants are determined over a range in temperature, leading to accurate Arrhenius parameters for both reactions. The reasons for such a study are twofold. First, $k_1(T)$ can be extrapolated to temperatures which are inaccessible experimentally. These include flame temperatures in excess of 1500 K, and the low temperatures found in the upper atmosphere (140–240 K), where k_1 is too slow to measure in the laboratory because of its large endothermicity ($\Delta H^\circ = 21.5 \text{ kJ mol}^{-1}$).¹³ The interest in sodium compounds in the stratosphere stems from the following consideration. The major source of atmospheric sodium is meteoritic¹⁴ and a layer of free atomic Na has been observed a few kilometers wide at an altitude of about 90 km.¹⁵ A number of recent atmospheric models¹⁶⁻¹⁸ have concluded that beneath this layer Na will be present principally as NaO_2 , NaOH , and NaHCO_3 . As these compounds diffuse down through the upper atmosphere they will react extremely rapidly with HCl to form NaCl.^{19,20} NaCl photolyzes readily in the stratosphere,²¹ and so this series of reactions represents a sensitized photolysis of HCl to Cl atoms which are then in an active form to destroy ozone in a catalytic cycle.²² This may be an important effect because HCl is the major sink of chlorine in the stratosphere.²² However, the efficiency of this process depends on NaCl surviving in the gas phase. In fact, polymerization of NaCl may be sufficiently rapid to provide a permanent reservoir for both Na and Cl.²² Also, the reaction



may be reasonably fast at 200 K, and thus alter the balance between NaCl and HCl in the upper stratosphere where the H atom concentration is relatively large.²³ In this study, $k_{-1}(200\text{ K})$ will be obtained through detailed balancing with $k_1(200\text{ K})$.

The second reason for studying reactions (1) and (2) is because of their interesting reaction dynamics. The molecular dynamics of reaction (1) have been studied in some detail. Bartoszek *et al.*⁴ used an infrared chemiluminescence depletion method to show that the cross section of reaction (1) increased by several orders of magnitude, equivalent to a collision efficiency of near unity, when the HCl was vibrationally excited. From this evidence they conjectured that the potential surface for the reaction must exhibit a late barrier, with no extension into the entrance valley. Weiss *et al.*⁵ in a recent paper demonstrated that electronic excitation of the Na led to a dramatic increase in reaction cross section. This was explained in terms of the smaller ionization energy of the excited Na atoms increasing the likelihood of the reaction occurring via the "harpoon" mechanism, at least for nearly linear Na–Cl–H approach geometries.⁵ In a preliminary investigation of reaction (1), Marshall and Husain⁶ observed Arrhenius behavior of the reaction over a limited temperature range (720–780 K), but an unexpected decrease in $k_1(T)$ at higher temperatures. Reaction (2) does not appear to have been studied previously.

Figure 1 illustrates the energies involved along the en-

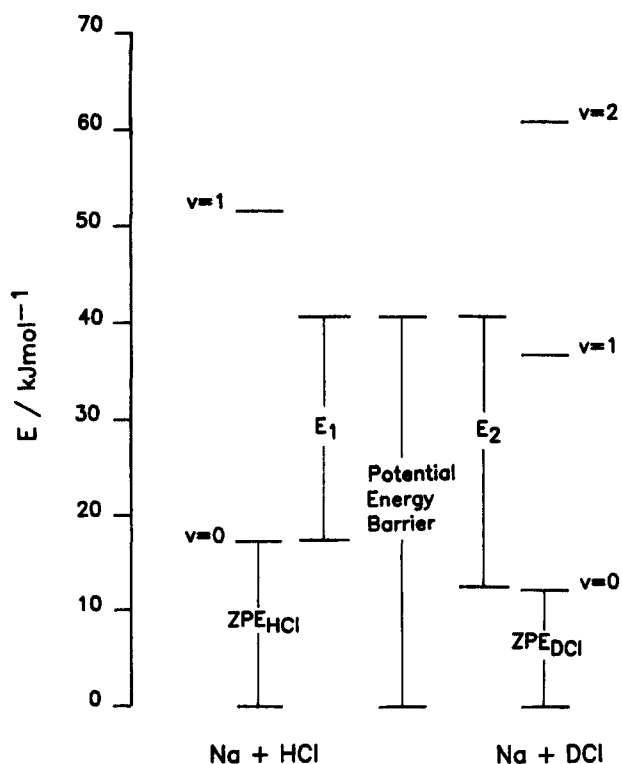


FIG. 1. The relative energies in the entrance channels of the reactions Na + HCl and Na + DCl. The energy of the potential barrier is taken from Refs. 4 and 5. The vibrational levels of HCl and DCl are labelled with the quantum number v . ZPE = zero-point energy. E_1 and E_2 are the reaction energy barriers for Na + HCl and Na + DCl, respectively, excluding the zero-point energies of the transition states.

trance channels of reactions (1) and (2). The molecular beam study of Weiss *et al.*⁵ demonstrated that the reactants require at least 23.4 kJ mol^{-1} of translational energy for reaction to occur. Thus, the potential energy barrier is probably about 41 kJ mol^{-1} above the potential energy minimum of the reactants.^{4,5} Including the zero-point energies of the reactants¹³ and neglecting the zero-point energies of the transition states (which will be relatively small for these reactions with late barriers), the reaction energy barriers (E_1 and E_2 in Fig. 1) are then about 23 and 29 kJ mol^{-1} for reactions (1) and (2), respectively. As indicated in Fig. 1, there is sufficient energy in $\text{HCl}(v=1)$ (33.3 kJ mol^{-1} ¹³) to surmount E_1 and turn on the reaction even if the translational energy is small. In view of the demonstrated vibrational enhancement of the reaction,⁴ the activation energy measured in the present study should reflect the size of this vibrational quantum and include a small amount of translational energy required to bring the reactants together, i.e., the activation energy should be close to 40 kJ mol^{-1} and thus significantly larger than the energy barrier, which is a rather unusual circumstance.

For reaction (2), the situation is even more interesting. Reaction (2) is likely to be greatly enhanced by the vibrational excitation of DCl. However, $\text{DCl}(v=1)$ (25.0 kJ mol^{-1} ¹³) does not possess sufficient energy to surmount E_2 , and so a modest amount of reactant translational energy will be required for successful reaction. By contrast, the reaction with $\text{DCl}(v=2)$ (49.4 kJ mol^{-1} ¹³) is expected to proceed with the minimum of translational energy. The objective here is to determine whether the state-specific reaction Na + $\text{DCl}(v=1)$ has a sufficiently large cross section to dominate reaction 2 over the temperature range of this study; in that case, the activation energy for reaction 2 would be lower than that of reaction (1). This would be a most unusual example of a reverse kinetic isotope effect, since the smaller zero-point energy of DCl normally results in reactions of DCl exhibiting larger activation energies than the analogous reactions of HCl.²⁵

The experimental study in this paper is followed by a theoretical investigation of reactions (1) and (2). *Ab initio* potential energy surfaces are first generated at the Hartree-Fock (HF) level, as fixed-angle cuts through the lowest $^2A'$ hypersurface. Fourth-order Moller-Plesset (MP4) perturbation theory²⁴ calculations at the stationary points on each PES are next employed to correct the surfaces for electron correlation. The surfaces are then adjusted to yield experimentally correct dissociation limits along the reaction coordinates. Finally, quasiclassical trajectories are run on the collinear PES, for computational simplicity, in order to demonstrate the effects of reagent vibrational excitation on the course of reactions (1) and (2).

II. EXPERIMENTAL STUDY

A. Experimental technique

Reactions (1) and (2) were investigated by the technique of time resolved laser induced fluorescence spectroscopy of Na atoms following the pulsed photolysis of NaCl vapor in an excess of HCl/DCl and He bath gas. The experi-

mental system has been described in detail elsewhere.^{7,26} Briefly, the reactions were studied in a stainless steel reactor consisting of a central cylindrical reaction chamber at the intersection of two sets of horizontal arms which cross orthogonally. These arms provide the optical coupling of the laser and the flash lamp to the central chamber where the reactions are initiated, as well as the means by which the flows of the reagents and the bath gas enter the chamber. The central chamber is enclosed in a furnace which can heat it to over 1100 K. The temperature of the gas in the central chamber is monitored by a permanently inserted chromel-alumel thermocouple in an inconel sheath, situated about 1 cm below the reaction volume in the center of the reactor. One of the sidearms is independently heated to act as a heat-pipe source of NaCl vapor, which has a large photolysis cross-section below 300 nm.^{21,27} Powdered NaCl was placed in a tantalum boat in the heat pipe and then heated to about 850 K, where the concentration of the NaCl vapor in equilibrium above the molten salt is $2.0 \times 10^{13} \text{ cm}^{-3}$.¹³ The vapor was then entrained in a flow of He and carried into the central chamber, where it was photolyzed by a small flash lamp (EG&G, Model FX193U). A fifth vertical side arm provides the coupling for the photomultiplier tube (Thorn EMI Gencom Inc., Model 9816QB) which monitors the LIF signal. The Na atoms were selectively pumped on one of the *D* lines at $\lambda = 589.0 \text{ nm}$ [$\text{Na}(3^2P_{3/2}) - \text{Na}(3^2S_{1/2})$] using a nitrogen-pumped dye laser (Laser Science Inc, Model VSL-337; laser dye Rhodamine-6G, bandwidth $\approx 0.01 \text{ nm}$). Fluorescence was measured from both upper states at $\lambda = 589.0, 589.6 \text{ nm}$ [$\text{Na}(3^2P_{3/2,1/2}) - \text{Na}(3^2S_{1/2})$] after passing through an interference filter centered at 589 nm (Oriol Corporation, fwhm = 10 nm). The LIF signal was then captured using a gated integrator (Stanford Research Systems, model SR250) interfaced to a microcomputer.

The procedure we used previously⁷ for passivating the surface of the reaction vessel with HCl was adopted here, although the concentrations of HCl/DCl were much higher in this study and wall losses did not appear to be significant.

The upper range in temperature ($\approx 820 \text{ K}$) was constrained by the rapid approach to equilibrium in both reactions (see below). The lower temperature limit ($\approx 580 \text{ K}$) was constrained by the requirement to generate a sufficient concentration of NaCl vapor in the reaction vessel to yield a S/N upon photolysis of more than 5:1. As before,⁷ we tried using NaI as a precursor, since this is both more volatile and has a much larger photolysis cross section in the near UV than NaCl,²⁷ but found significant halogen exchange with the HCl in the central chamber.

1. Materials

Helium, 99.9999% (Matheson "Matheson Purity") was used without further purification. NaCl, 99% (Aldrich, anhydrous) was refluxed in the reactor side arm at 700 K for several hours prior to kinetic experiments, to remove traces of Cl_2 . HCl, 99.0% (Matheson, Technical Grade) was refluxed from 155 K (ethanol slush) to 77 K (liquid nitrogen) repeatedly before use. DCl was made by the action of D_2O on SiCl_4 and then purified by refluxing from 155 to 77 K.²⁵

B. Experimental results

Under the conditions of the present study, in which the concentration of HCl or DCl was always well in excess of the concentration of Na resulting from the pulsed photolysis of NaCl vapor, the loss of Na atoms should be described by the pseudo first-order decay coefficient k' where

$$k' = k_{\text{diff}} + k_1 \cdot [\text{HCl}] \text{ or } k_2 \cdot [\text{DCl}]. \quad (3)$$

The term k_{diff} describes diffusion of the Na atoms out of the volume defined by the intersection of the beams from the flashlamp and the dye laser and within the field of view of the PMT.²⁶ Below 820 K, the observed decays of the LIF signal at $\lambda = 589 \text{ nm}$ were indeed of a simple exponential form, $A \cdot \exp(-k't)$. Figure 2 illustrates plots of k' against $[\text{HCl}]$ at a selection of the temperatures studied, demonstrating a clear linear dependence. At 738 K, two sets of data at total

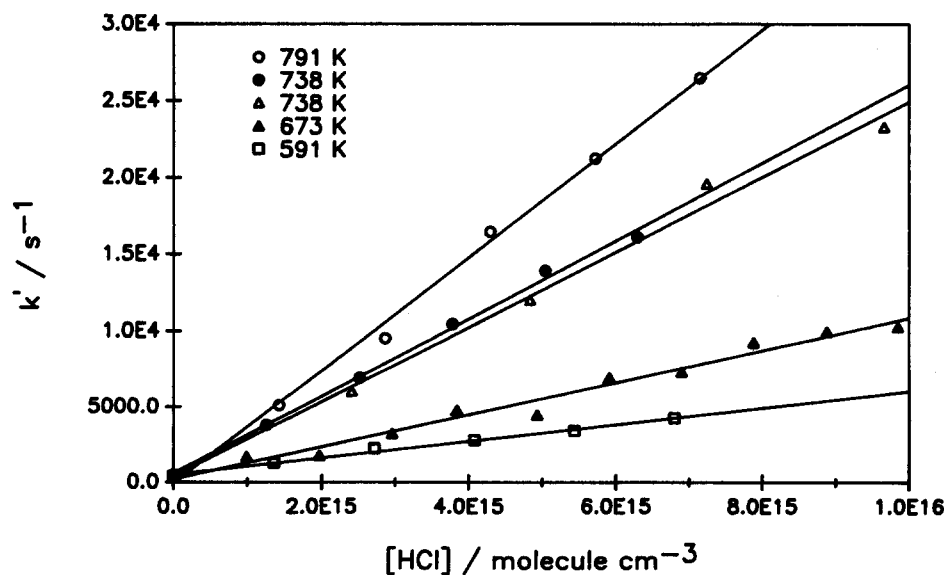


FIG. 2. Plots of the pseudofirst-order rate coefficient (k') against $[\text{HCl}]$ over a range of temperatures. Solid lines are linear least-squares fits to the data. The two sets of measurements at 738 K were made at pressures of 21.0 (●) and 40.0 (△) Torr.

pressures of 21.0 and 40.0 Torr were recorded. As shown in Fig. 2, there is no significant effect of pressure on k_1 , as expected. The slopes of such plots thus yield k_1 and k_2 as a function of temperature, listed in Table I with 2σ errors from a linear regression fit to each plot.

Figure 3 illustrates standard Arrhenius plots of the data for reactions (1) and (2) contained in Table I. A linear regression fit to each plot yields

$$k_1(\text{Na} + \text{HCl}) = (2.1 \pm 0.5) \times 10^{-9} \times \exp[(-41.8 \pm 1.5 \text{ kJ mol}^{-1})/RT] \text{ cm}^3 \text{ molecule}^{-1} \text{ s}^{-1}, \quad (4)$$

$$k_2(\text{Na} + \text{DCI}) = (2.2 \pm 1.0) \times 10^{-9} \times \exp[(-45.5 \pm 3.8 \text{ kJ mol}^{-1})/RT] \text{ cm}^3 \text{ molecule}^{-1} \text{ s}^{-1}. \quad (5)$$

The quoted errors are 2σ , calculated from the absolute errors in Table I.

Figure 4 illustrates the decay of the LIF signal at 589 nm [$\text{Na}(3^2P_j - 3^2S_{1/2})$], generated by the pulsed photolysis of NaCl in the presence of DCl at 853 K. The decay is clearly not of the simple exponential form observed at lower temperatures. The initial rapid decay of Na is consistent with the removal of Na by reaction (2), followed by a much slower rate of decay. We believe this is evidence for reaction (2) proceeding until equilibrium is achieved with the reverse reaction,



The slow loss of Na is then actually due to the diffusion of D atoms out of the reaction volume probed by the dye laser, since the diffusion coefficient of D atoms will be about 5 times faster than the diffusion coefficient of Na at elevated temperatures,²⁸⁻³⁰ and both species are coupled through the equilibrium (2), (-2). This effect, which was also observed

TABLE I. Experimental determinations of $k_1(\text{Na} + \text{HCl})$ and $k_2(\text{Na} + \text{DCI})$ as a function of temperature (2σ errors).

$k_1(10^{-13} \text{ cm}^3 \text{ molecules}^{-1} \text{ s}^{-1})$	T/K
4.71 ± 0.82	591
6.62 ± 0.30	613
6.14 ± 0.21	621
8.74 ± 0.34	643
7.87 ± 0.24	644
10.5 ± 0.9	673
14.1 ± 0.1	686
17.3 ± 1.6	711
20.6 ± 1.6	724
20.2 ± 1.8	738
25.4 ± 2.2	738
22.7 ± 1.6	741
27.2 ± 1.8	751
31.0 ± 2.0	756
35.1 ± 2.9	773
37.0 ± 2.6	791
$k_2(10^{-13} \text{ cm}^3 \text{ molecule}^{-1} \text{ s}^{-1})$	T/K
2.93 ± 0.28	605
4.45 ± 0.29	650
6.87 ± 0.41	680
8.71 ± 0.60	698
11.9 ± 0.8	726
15.0 ± 1.1	743
17.1 ± 2.0	766
21.7 ± 1.9	783
28.7 ± 2.8	821

for reaction (1) above 800 K, limits the maximum temperatures at which these reactions can be studied. On the other hand, at temperatures below 800 K in the central chamber only a tiny fraction²⁶ of the NaCl vapor entering from the independently heated side-arm source reaches the reaction volume in the center of the chamber, because of condensa-

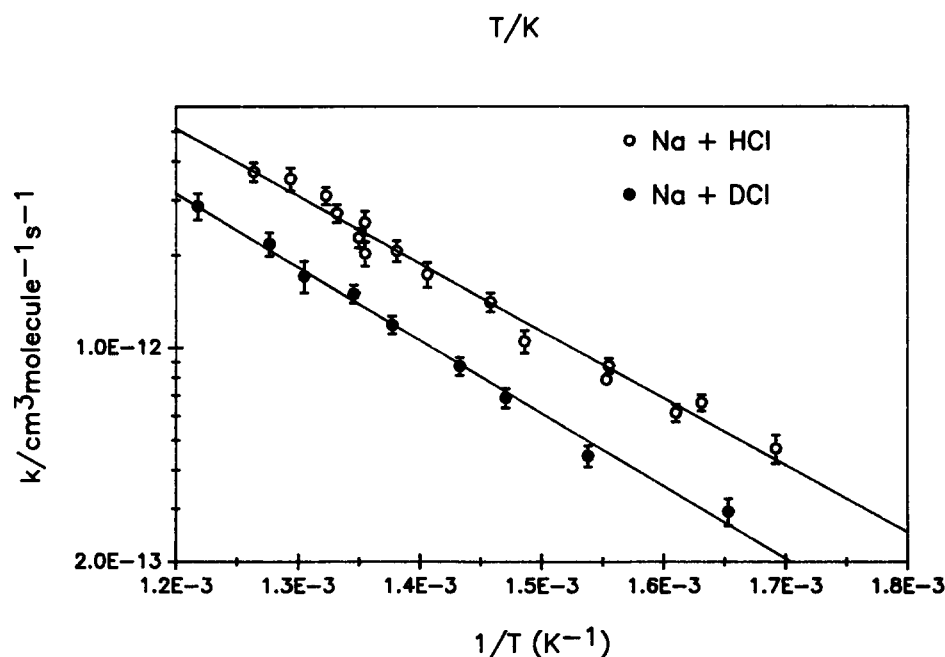


FIG. 3. Standard Arrhenius plots [$\ln k(T)$ vs $1/T$] over the temperature range 590–820 K, for the reactions Na + HCl and Na + DCI. Error bars depict 2σ errors from the least-squares fits to the data of plots exemplified in Fig. 2. The solid lines are regression curves through the sets of experimental data.

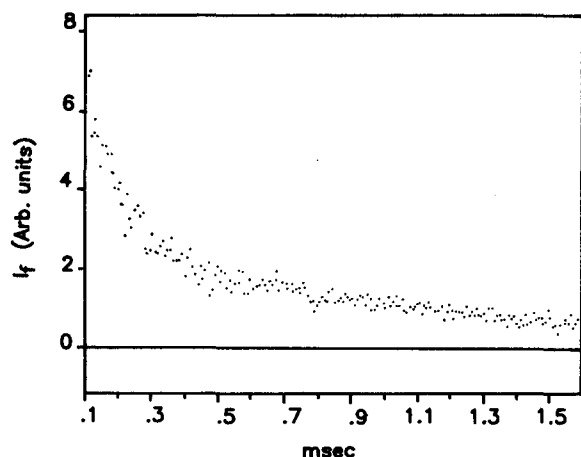


FIG. 4. Time-resolved decay of the LIF signal from Na atoms at $\lambda = 589$ nm [$\text{Na}(3^2P_{3/2,1/2})-\text{Na}(2^2S_{1/2})$] following the pulsed photolysis of NaCl vapor in DCl and He; $[\text{DCl}] = 1.42 \times 10^{15}$ molecule cm^{-3} ; $[\text{He}] = 2.81 \times 10^{17}$ cm^{-3} , $T = 853$ K.

tion on the cooler reactor walls. Thus, even though the equilibrium constant for reactions (1) and (2) becomes less favorable at lower temperatures, the forward reaction dominates because of the very low NaCl vapor concentrations.

Following our previous procedure,⁷ the decay in Fig. 4 can be analyzed to estimate the equilibrium constant, $K_2(853 \text{ K}) = 0.0774$. Equating this value with a statistical mechanical expression for $K_2(853 \text{ K})$ with molecular parameters taken from Ref. 13, yields ΔH_0° [reaction (2)] = 24.4 kJ mol^{-1} . This compares very satisfactorily with a value of 26.5 kJ mol^{-1} , calculated using the bond energies for DCl and NaCl.¹³

TABLE II. Asymptotic properties^a of the potential energy surface.

	$r_e(\text{HCl})$	$\nu_e(\text{HCl})$	$r_e(\text{NaCl})$	$\nu_e(\text{NaCl})$	$D_e(\text{HCl})$ - $D_e(\text{NaCl})$
Expt. ^b	1.275	2890	2.361	364	37.2
HF/6-31G*	1.266	3188	2.397	359	9.3
HF/6-31G	1.295	2925	2.434	341	-16.5
HF/6-31 + G	1.297	2917	2.444	333	-32.9

^aBond lengths in Å, vibrational frequencies in cm^{-1} , bond energies in kJ mol^{-1} .

^bTaken from Ref. 13.

III. THEORETICAL STUDY

A. Generation of potential energy surfaces

One challenge in generating potential energy surfaces for the class of alkali atom-hydrogen halide reactions is to find a basis set which adequately describes both the covalent reactants and ionic products.³¹ We examined a number of the standard split-valence basis sets available within the GAUSSIAN 86 set of programs.³² Based on a comparison of the experimental bond lengths and vibrational frequencies of HCl and NaCl and the reaction endothermicity,¹³ with those properties calculated from a set of SCF optimizations, the 6-31G* basis set was found to be most satisfactory. This comparison is illustrated in Table II. The 6-31G* basis set includes single first polarization functions by placing d orbitals on the Na and Cl atoms. The 6-31G* basis set also gave a better estimate of the reaction endothermicity than the more flexible 6-311G* set [HF/6-311G* yields $D_e(\text{HCl}) - D_e(\text{NaCl}) = -0.1 \text{ kJ mol}^{-1}$]. Note that the other possible reaction channel, $\text{Na} + \text{HCl} \rightarrow \text{NaH} + \text{Cl}$ ($\Delta H_0^\circ = 245.8 \text{ kJ mol}^{-1}$),¹³ is much too endothermic to play a role over

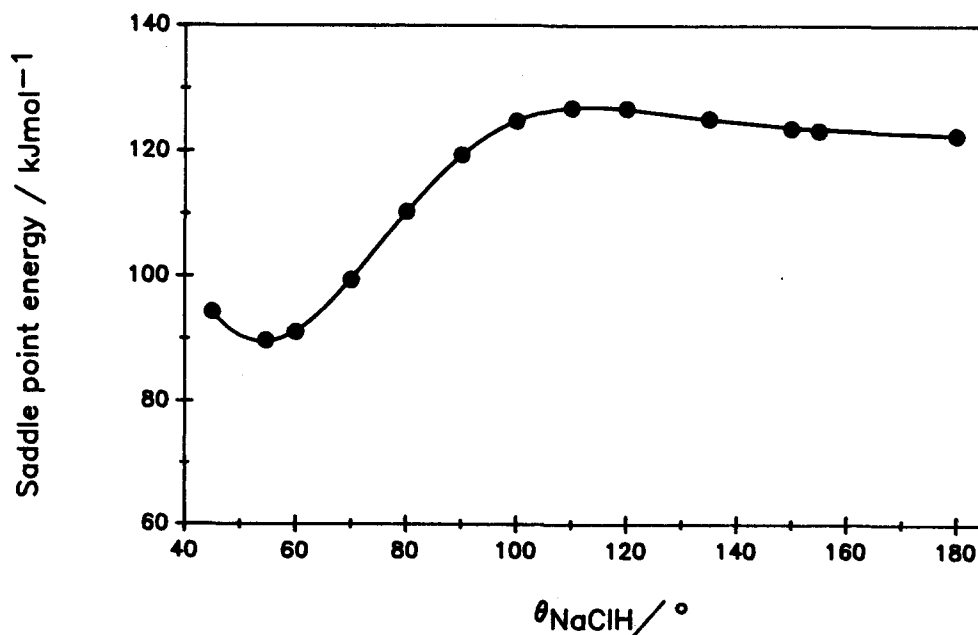


FIG. 5. A plot of the variation of the saddle point energy relative to the reactant potential energy for the reaction $\text{Na} + \text{HCl}$, as a function of fixed Na-Cl-H angle. The saddle energies were calculated by transition state optimizations at the HF/6-31G* level.

TABLE III. Characteristics^a of stationary points on the 6-31G* PES.

Geometry	$r(\text{HCl})^a$	$r(\text{NaCl})^a$	θ_{NaClH}^a	γ_c	$E(\text{UHF})^a$	$E[\text{MP4}(\text{SDTQ})]^a$
Na + HCl	1.266	20.0	180.00°	...	0	0
Na-Cl-H ^{†b}	1.616	2.595	180.00°	0.85	122.3	89.0
Na-Cl-H ^{†b}	1.565	2.634	54.66°	0.89	89.7	51.9
NaCl + H	2.397	20.0	180.00°	...	9.3	12.8

^aDistances in Å, energies in kJ mol⁻¹. The energy zero is set at the entrance channel.

^bSaddle points.

^cLocation of the saddle point. $\gamma = [r^\ddagger(\text{NaCl})/r^\ddagger(\text{HCl})]/[r_e(\text{NaCl})/r_e(\text{HCl})]$. $\gamma < 1$ indicates a barrier in the exit channel.

the range of thermal energies employed in the present experimental study.

The 6-31G* basis set was thus employed in the calculations of the full PES which follow. The set of minimum energy paths between reactants and products, defined as a function of the fixed Na-Cl-H angle hereafter termed θ , all contain saddle points. A selection of these saddle points were located by SCF transition state optimizations,³² and their relative energies are illustrated in Fig. 5 as a function of θ . The lowest saddle point on the ground state PES is located at $\theta^\ddagger = 54.7^\circ$. Presumably this bent configuration is stabilized by the partial formation of a Na-H bond. Figure 5 indicates that a collinear reaction pathway is also favorable, but with a saddle point of somewhat higher energy. The geometries of these two saddle points are listed in Table III, as well as the parameter γ describing the displacement of the saddle point with respect to the midpoint of the reaction coordinate (see footnote of Table III for a definition of γ). Both saddle points are in the exit channel, with $\gamma < 1$. The HF and MP4(SDTQ)³² energies of the two saddle points and the energies of the reaction products, relative to the reactants, are also listed in Table III. At the MP4 level, the endothermicity of the reaction is only slightly changed, but a significant lowering of both saddle points is evident relative to the HF energies. A similar improvement was noted in a recent *ab initio* study of the reaction Li + HCl.³¹ That study³¹ also demonstrated that the orbital superposition errors at the UHF level for the transition state of the analogous reaction are of the order of 4 kJ mol⁻¹. Superposition errors in the case of reaction (1) should also be small relative to the size of the reaction barrier. Note that even at the MP4 level, the calculated minimum saddle point is still about 10 kJ mol⁻¹ above the experimental barrier.^{4,5}

Table IV shows a comparison of the geometry and energy of the lowest saddle point on the ²A' PES calculated using

the 6-31G*, 6-31G and 6-31 + G basis sets. The geometry of the saddle point is relatively basis set independent. The calculated saddle point energies are lower for the last two basis sets, and in fact equal to the experimental barrier in the case of the MP4/6-31 + G//HF/6-31 + G calculation. However, as already noted, these basis sets gave an increasingly poor estimate of the reaction endothermicity and overestimated the $r_e(\text{NaCl})$ bond length (Table II), so that the apparently good agreement of the saddle point energy is most likely an accidental result of the poor representation of the exit channel.

Potential energy surfaces were then constructed for $\theta = 180.0^\circ$ and 54.7° from 399 and 678 single-point HF/6-31G* calculations, respectively. These surfaces are illustrated using isoenergetic contours in Figs. 6(a) and 6(b), respectively. Two modifications were then made to both surfaces. First, the HF surfaces were corrected to agree with the calculated heights of the saddle points at the MP4 level (Table III). This was achieved by subtracting a Gaussian term with an amplitude of 33.3 or 37.8 kJ mol⁻¹, respectively, centered on the saddle point in each case. The width of the Gaussians was limited so that this correction only affected the immediate vicinities of the saddle points. The second correction was applied to reproduce the experimental endothermicity (37.2 kJ mol⁻¹¹³). This entailed adding a term to the asymptotic region of the exit channel which decayed exponentially towards the saddle point. Both of these types of corrections to a PES are described in detail elsewhere.^{31,33} The final surfaces are illustrated in Figs. 6(c) and 6(d).

B. Quasiclassical trajectory studies

These studies were carried out primarily to illustrate the role of vibrational excitation in turning on the reaction, and are not an exhaustive dynamical investigation over the com-

TABLE IV. Comparison of the lowest saddle point on the ²A' PES as a function of basis set.

Basis set	$r^\ddagger(\text{HCl})^a$	$r^\ddagger(\text{NaCl})^a$	γ^b	$\theta_{\text{NaClH}}^\ddagger^a$	$E(\text{UHF})^a$	$E[\text{MP4}(\text{SDTQ})]^a$
6-31G*	1.565	2.634	0.89	54.66°	89.7	51.9
6-31G	1.561	2.784	0.95	52.75°	66.7	44.1
6-31 + G	1.560	2.796	0.95	52.21°	65.7	41.6

^aDistances in Å, energies in kJ mol⁻¹. The energy zero is set at the entrance channel.

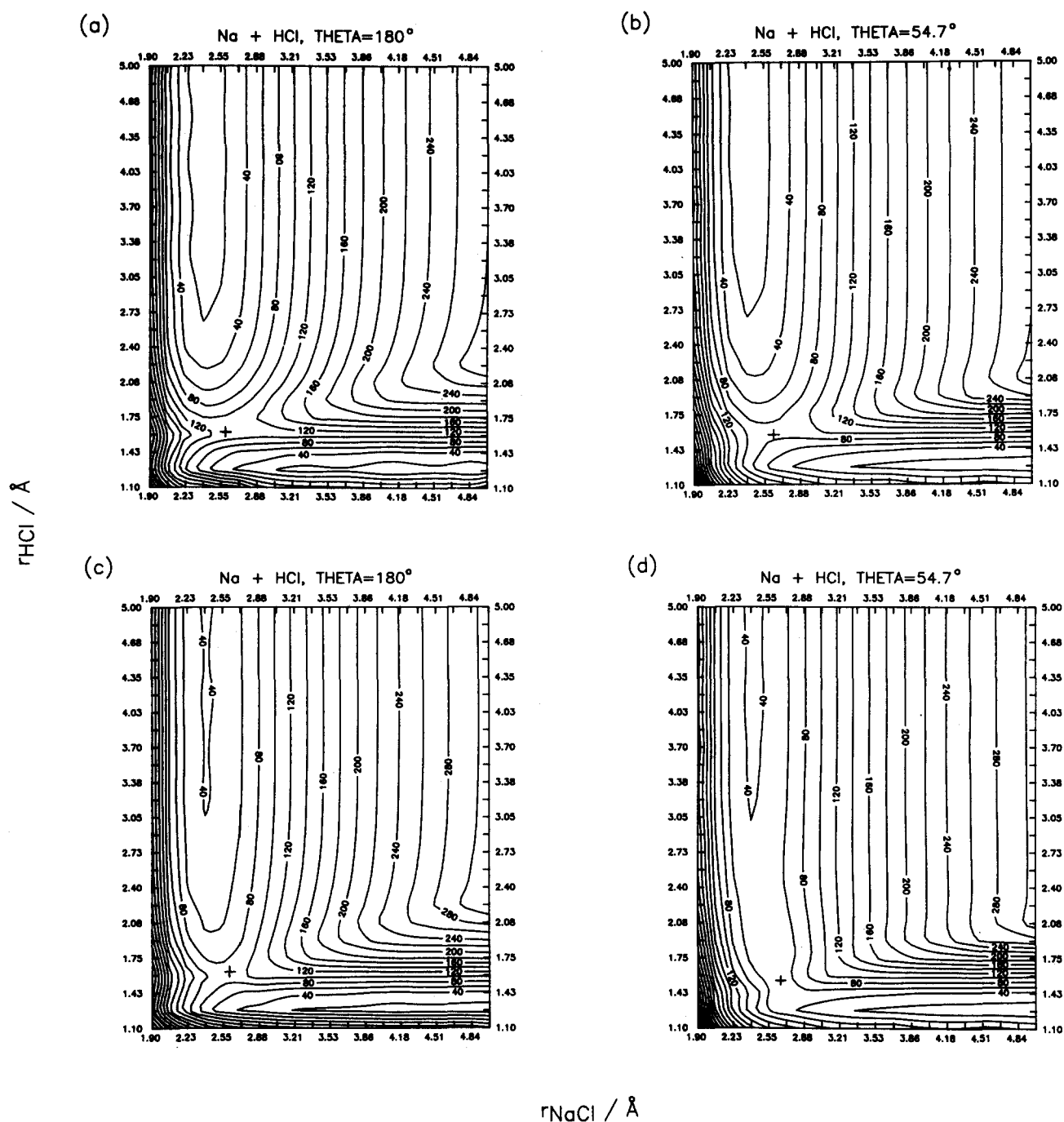


FIG. 6. A set of potential energy surfaces for the reaction Na + HCl at fixed Na-Cl-H angle slices through the hypersurface, plotted as isoenergetic contours with a spacing of 20 kJ mol^{-1} and bond distances in \AA : (a) collinear surface, calculated at the HF/6-31G* level; (b) the surface containing the lowest saddle point on the ${}^2A'$ hypersurface, calculated at the HF/6-31G* level; (c) and (d) surfaces derived from (a) and (b), respectively, by correcting the saddle points to the MP4/6-31G**//HF/6-31G* level energies and adjusting the exit channel to give the experimental reaction endothermicity (see the text). The saddle points on the four surfaces are marked with a cross.

plete hypersurface. For computational simplicity, and in view of the experimental evidence⁵ that reaction (1) appears to proceed at low energies via a collinear transition state, we performed the trajectory calculations on the collinear surface [Figure 6(c)]. Reactive trajectories were run from the saddle point in the forwards and backwards directions. Most trajectories were initialized with 4 kJ mol^{-1} of internal energy above the saddle point. Examples of such trajectories are

illustrated in Fig. 7, for reactions (1) and (2). These trajectories are shown starting in the entrance channel, where the HCl or DCl is clearly vibrationally excited.

The reactant energies for these trajectories are listed in the caption to Fig. 7. Smith³⁴ has described a quasiclassical procedure for quantizing the internal energies of the reactants in a classical trajectory calculation. For example, if the vibrational energy of the HCl, after running a trajectory

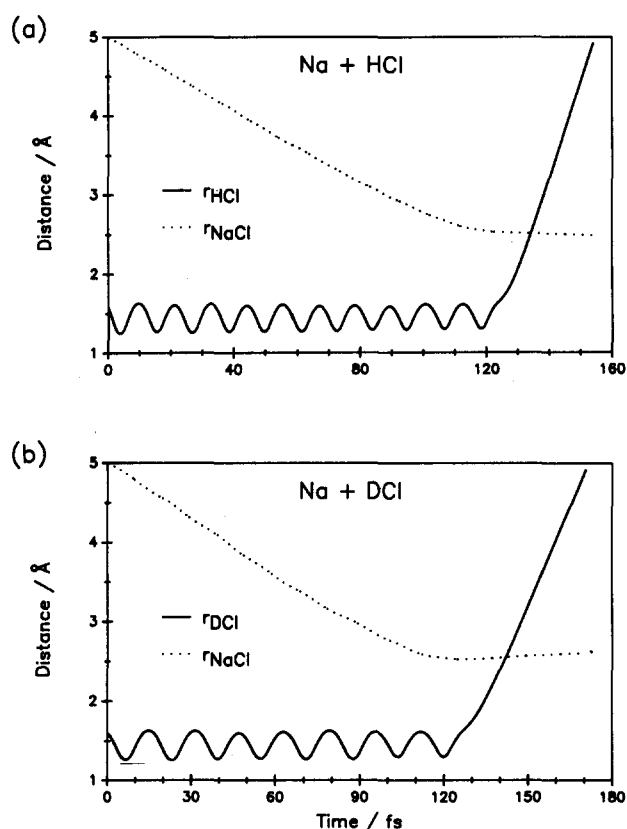


FIG. 7. Reactive classical trajectories calculated for Na + HCl and Na + DCl collisions on the collinear surface illustrated in Fig. 6(c). The internal energy at the saddle point was 4 kJ mol^{-1} for both trajectories: (a) the reaction Na + HCl, with initial energies $E_{\text{trans}} = 38 \text{ kJ mol}^{-1}$, $E_{\text{vib}} = 55 \text{ kJ mol}^{-1}$; (b) the reaction Na + DCl, with initial energies $E_{\text{trans}} = 42 \text{ kJ mol}^{-1}$, $E_{\text{vib}} = 51 \text{ kJ mol}^{-1}$.

backwards to the start of the entrance channel, lies between $(\omega_e - \omega_e x_e)$ and $[2\omega_e - (2)^2 \omega_e x_e]$ where ω_e is the vibrational fundamental frequency and $\omega_e x_e$ is the vibrational anharmonicity constant,¹³ then the HCl is assumed to be in the $v = 1$ state. The vibrational energy in Figure 7(a) corresponds to $\text{HCl}(v = 1)$, while that in Fig. 7(b) falls just within $\text{DCl}(v = 2)$. Trajectories were also run from the saddle point with internal energies up to 40 kJ mol^{-1} , in order to examine the relative importance of vibrational as opposed to translational reactant energy in the entrance channel. The implications of these calculations are discussed below.

IV. DISCUSSION

The diffusion flame work that was carried out on reaction (1) in the 1930s³⁵⁻³⁸ has been critically reviewed by Husain and Marshall⁶ in terms of their recent direct measurements of $k_1(T)$. Their study⁶ employed the technique of flash photolysis of NaCl vapor followed by time-resolved resonance absorption of Na atoms to obtain the Arrhenius expression: $k_1(719-783 \text{ K}) = (4 \pm 7) \times 10^{-10} \exp[-(34 \pm 6 \text{ kJ mol}^{-1})/RT] \text{ cm molecule}^{-1} \text{ s}^{-1}$ (1σ errors). A comparison with the present study [Eq. (4)] indicates only fair agreement at the 2σ error level. In fact, the two studies agree well at $k_1(700 \text{ K})$, but at

higher temperatures the values of $k_1(T)$ in the study of Husain and Marshall⁶ fall increasingly below our data points, and actually decrease with increasing temperature above 820 K . Those authors⁶ discussed the possibility of thermal decomposition of the reactants in their quartz reactor above 820 K causing this decrease. As noted above, we observed a similar apparent decrease in our measured rate constants above 820 K , which we demonstrated was caused by the rapid approach to equilibrium of reactions (1) and (2) (see Fig. 4) by working at shorter time scales than was possible in the study of Husain and Marshall.⁶

The activation energy for reaction (1) obtained in this study may be shown by the following argument to be in good accord with the two recent studies of Bartoszek *et al.*⁴ and Weiss *et al.*⁵ The latter study⁵ concluded that the reaction cross section for $\text{Na}(3^2\text{S}) + \text{HCl}(v = 0)$ was very small (in the range $0.0034-0.057 \text{ \AA}^2$) when the reactants possessed just sufficient translational energy (23.4 kJ mol^{-1}) to surmount the reaction barrier E_1 . By contrast, Bartoszek *et al.*⁴ demonstrated that vibrational excitation of HCl increases the reactive collision efficiency to near unity. Thus, over the temperature range of the present experiments ($590-790 \text{ K}$), the contribution to the observed loss of Na in reaction (1) from reaction of $\text{HCl}(v > 1)$ is about 100-1000 times greater than that of $\text{HCl}(v = 0)$. Note that the thermal distribution of vibrational states of HCl is maintained during the reaction because the Na atom concentration produced by the flash is always less than 1% of $[\text{HCl}(v > 1)]$. We therefore make the simplifying assumption that, over the temperature range of this study, reaction (1) occurs exclusively from vibrationally excited reagents. The activation energy for reaction (1) will then be the sum of three components: a quantum of vibrational energy (34.5 kJ mol^{-1} ¹³), representing the probability that the HCl is vibrationally excited, i.e., $P(v > 1, T) = \exp(-34.5 \text{ kJ mol}^{-1}/RT)$; the translational energy ($\sim 4.2 \text{ kJ mol}^{-1}$) that Bartoszek *et al.*⁴ have shown is required to bring the Na and $\text{HCl}(v > 1)$ reactants together to the region of strong interaction; and the factor $0.5 RT$ (2.8 kJ mol^{-1} at 700 K , the midrange of our study) describing the temperature dependence of the collision frequency.³⁹ That is, the activation energy should be about 41.5 kJ mol^{-1} , comparing very well with our measured value of 41.8 kJ mol^{-1} .

One striking feature of the Arrhenius expressions (4) and (5) is their large pre-exponential factors, which are about a factor of 2.4 times larger than the collision frequency between Na and HCl at 700 K (see below). The possibility of an experimental artifact can be discounted on several grounds: the good agreement between our value of k_1 (700 K) and that measured by Husain and Marshall⁶ using a different technique; the very good estimate of the endothermicity of reaction 2 from analysis of the observed equilibrium at 850 K (see above—Fig. 4), which is sensitive to k_2 (850 K) obtained from the Arrhenius expression (5); and finally, the observation that the activation energy for reaction (1) appears to be in excellent accord with the study of Bartoszek *et al.*⁴ so that any systematic error in our experimental rate constants would be temperature independent and hence unlikely. In fact, we have previously²⁶ observed a pre-exponen-

tial factor in excess of the collision number for the reaction $\text{Li} + \text{N}_2\text{O}$ over the temperature region above 600 K where N_2O is significantly populated vibrationally. This reaction is analogous to the present reactions in that vibrational excitation of N_2O is thought to greatly enhance the rate.²⁶ In that study²⁶ we also observed marked curvature in the Arrhenius plot over a larger temperature range (360–900 K) than was possible in the present study. By analogy, in the case of reactions (1) and (2) the slopes of the Arrhenius plots probably become less negative below 600 K as the vibrational enhancement of the reaction rates becomes insignificant, leading to both smaller activation energies and preexponential factors.

It follows from the assumption that reaction (1) proceeds almost exclusively from vibrationally excited HCl over our experimental temperature range, that the rate coefficient for the reaction of $\text{Na} + \text{HCl}(v \geq 1)$ is given by

$$k_1(v \geq 1, T) = k_1(T)/P(v \geq 1, T). \quad (6)$$

Thus, at 700 K and taking $k_1(700 \text{ K})$ from Eq. (4), $k_1(v \geq 1, 700 \text{ K}) = (6.1 \pm_{2.4}^{4.0}) \times 10^{-10} \text{ cm}^3 \text{ molecule}^{-1} \text{ s}^{-1}$. This rate coefficient should be compared with the collision frequency between Na and HCl at 700 K, estimated in terms of the orbiting criteria on the attractive surface due to the long-range interaction between the reactants.^{7,34} The dispersion coefficient $C_6^{\text{disp}} = 2.25 \times 10^7 \text{ J } \text{\AA}^6$ may be calculated from the Slater–Kirkwood formula⁴⁰ using a polarizability for Na ($\alpha_{\text{Na}} = 27.59 \times 10^{-24} \text{ cm}^3$) derived from the present set of *ab initio* calculations at the HF/6-31G* level, and a polarizability for HCl from Ref. 40. The dipole-induced dipole coefficient, $C_6^{\text{ind}} = 1.94 \times 10^6 \text{ J } \text{\AA}^6$, is calculated using the dipole moment of HCl from Ref. 41. Then the total long-range C_6 coefficient is given by $C_6^{\text{ind}} + C_6^{\text{disp}}$, and the collision frequency is estimated³⁴ to be $Z(700 \text{ K}) = 8.9 \times 10^{-10} \text{ cm}^3 \text{ molecule}^{-1} \text{ s}^{-1}$. Thus, $k_1(v \geq 1, 700 \text{ K})$ is about 70% of $Z(700 \text{ K})$, implying that reaction (1) proceeds with almost unit collision efficiency when the HCl is vibrationally excited.

The reaction cross section for vibrationally excited HCl, $\sigma(v \geq 1)$, may be obtained by the approximate relationship

$$k_1(v \geq 1, T) = \sigma(v \geq 1) \cdot \langle v, T \rangle, \quad (7)$$

where $\langle v, T \rangle$ is the root mean square collision velocity at T .³⁴ Thus we obtain $\sigma(v \geq 1) = (59 \pm 32) \text{ \AA}^2$, which is in reasonable agreement with the indirect estimates of $\sigma(v = 1) = (12 \pm 7) \text{ \AA}^2$ to $\sigma(v = 4) = (35 \pm 20) \text{ \AA}^2$ from the study of Bartoszek *et al.*⁴ Those authors⁴ rationalized these large reaction cross sections by using an electron jump model⁴² and discussed the manner in which vibrational excitation of the hydrogen halide would alter its electron affinity and hence its reactivity. Weiss *et al.*⁵ have argued that the large cross sections they have measured for the reactions $\text{Na}(3^2P, 4^2D, 5^2S) + \text{HCl}(v = 0)$ can be explained by the very low ionization potentials of the excited Na atoms increasing the crossing radius of the covalent and ionic curves. Although there is experimental evidence⁵ that an electron jump takes place on the excited electronic surfaces, the use of this model to explain the dynamics on the ground state surface is not satisfactory.⁴³ In fact, the present *ab initio* calcula-

TABLE V. Mulliken charges on the atoms at stationary points on the 6-31G* PES

	q_{Na}	q_{Cl}	q_{H}
Na + HCl	0.000	-0.195	0.195
Na–Cl–H, $\theta_{\text{NaClH}}^{\ddagger} = 54.66^\circ$	0.415	-0.445	0.030
Na–Cl–H, $\theta_{\text{NaClH}}^{\ddagger} = 180.0^\circ$	0.345	-0.355	0.010
NaCl + H	0.668	-0.668	0.000

^aSaddle points.

tions show that a partial charge transfer has already occurred before the saddle point is reached. Table V records the Mulliken charges on the atoms at stationary points on the 6-31G* PES. The charge transfer begins at the end of the entrance valley, before the steep ascent to the saddle point in the exit channel. If an electron jump mechanism were operating on this ground state electronic surface, a long range electron transfer would be expected to cause immediate dissociation of the HCl,⁵ so that the saddle point would probably occur earlier.

The geometry of the lowest saddle point on the 6-31G* PES illustrated in Figs. 6(b) and 6(d) is in very close agreement with that obtained in the recent *ab initio* study of Gallo and Yarkony,¹² although we have obtained a saddle point energy at the MP4 level which is in better agreement with the experimental barrier.^{4,5} However, the height of the collinear saddle point in our study (89.7 kJ mol^{-1}) is probably rather high, especially in view of the experimental demonstration⁵ that collinear reactions tend to dominate at low collision energies. In terms of the trajectory calculations run on the collinear surface, collision energies of about 40 kJ mol^{-1} are then required in addition to reactant vibrational energy to surmount the reaction barrier. Although such energies are well above the normal range of thermal translational energies, the trajectory calculations exemplified in Fig. 7, in conjunction with the quasiclassical procedure used to bin the initial quantum states of the HCl or DCl,³⁴ illustrate several important points. First, because of the late barrier in the exit channel, the H/D–Cl bond only begins to break after the Na–Cl bond has almost completely formed. Second, vibrational excitation of the hydrogen halide is critical to successful reaction. Indeed, none of the several hundred trajectories run backwards from the saddle point with different initial internal energies (ranging from 4–40 kJ mol^{-1}) reached the start of the entrance channel with less than one vibrational quantum in the reactants. Thirdly, the trajectories for reaction 2 indicate that the reaction is turned on by $\text{DCl}(v = 2)$ rather than $\text{DCl}(v = 1)$. This is probably reflected in the measured activation energy of $45.5 \pm 3.8 \text{ kJ mol}^{-1}$ for reaction (2), which is well above the first vibrational quantum of DCl (25.0 kJ mol^{-1} ¹³) and quite close to the second vibrational level (49.4 kJ mol^{-1} ¹³).

Finally, we draw attention to three discrepancies between the experimental work on reaction (1) in this study and elsewhere,^{4,5} and the results of the *ab initio* surface and trajectory calculations presented here. First, our PES calculations indicate that the reaction is favored through a very

bent transition state ($\theta_{\text{NaClH}} = 54.7^\circ$). In contrast to this finding and the theoretical result of Gallo and Yarkony,¹² Weiss *et al.*⁵ noted recently that the scattering distribution in their crossed molecular beam experiment implied a collinear or nearcollinear Na–Cl–H approach to reaction. Second, inspection of the surfaces in Fig. 6 indicates that significant translational energy is required to bring the reactants into the strong interaction zone, which is consistent with the results of the trajectory study (Fig. 7). This conflicts with the finding of Bartozcek *et al.*⁴ that only about 4 kJ mol⁻¹ of translational energy is needed for reaction when the HCl is vibrationally excited, which the measured activation energy in the present study appears to support. Third, the theoretical potential energy barriers calculated in this study and that of Gallo and Yarkony¹² are substantially higher than the experimental upper limit determined by Weiss *et al.*⁵ In fact, a similar discrepancy exists between the theoretical³¹ and experimental energy barriers^{7,45} for the analogous reaction Li + HCl. It appears that a higher level of *ab initio* calculations on the alkali + HCl systems will be required to remove these conflicts.

A. Extrapolation of k_1 and k_{-1} to atmospheric and flame temperatures

Equation (4) can be used to extrapolate $k_1(T)$ to the typical atmospheric and flame temperatures of 200 and 2000 K, respectively, yielding:

$$k_1(200 \text{ K}) = (2.6_{-1.8}^{+5.5}) \times 10^{-20} \text{ cm}^3 \text{ molecule}^{-1} \text{ s}^{-1},$$

$$k_1(2000 \text{ K}) = (1.7_{-0.5}^{+0.7}) \times 10^{-10} \text{ cm}^3 \text{ molecule}^{-1} \text{ s}^{-1}.$$

Detailed balancing by means of the equilibrium constant for reaction (1) calculated from the relevant molecular parameters in Ref. 13 and with $\Delta H_0^\circ = 21.5 \text{ kJ mol}^{-1}$, yields:

$$k_{-1}(200 \text{ K}) = (1.1_{-0.8}^{+2.3}) \times 10^{-14} \text{ cm}^3 \text{ molecule}^{-1} \text{ s}^{-1},$$

$$k_{-1}(2000 \text{ K}) = (1.8_{-0.5}^{+0.8}) \times 10^{-10} \text{ cm}^3 \text{ molecule}^{-1} \text{ s}^{-1}.$$

Thus, when Na is seeded into a chlorinated flame, the equilibrium between Na and NaCl will be established very rapidly. The possible atmospheric importance of reaction (–1) was outlined in the Introduction. Reaction (–1) can only play a role in the stratospheric chlorine cycle above 60 km, where the H atom concentration becomes significant ($[\text{H}] > 10^7 \text{ cm}^{-3}$). However, the atomic Na formed in reaction (–1) will recombine with O₂ in a very fast termolecular reaction,⁴⁴ and the resulting NaO₂ will in turn react rapidly with HCl to yield NaCl.¹⁹ Even allowing for reaction (1) to be strongly non-Arrhenius below 600 K (see above) and hence $k_{-1}(200 \text{ K})$ to be up to 2 orders of magnitude faster, the reaction is nevertheless too slow to influence appreciably the balance of chlorine between NaCl and HCl in the upper atmosphere.

ACKNOWLEDGMENTS

This work was supported by the National Science Foundation under Grant No. ATM-8616338, and a Faculty Research Support Award from the University of Miami.

- ¹M. Polanyi, *Atomic Reactions* (Williams and Norgate, London 1931): C. E. H. Bawn and A. G. Evans, *Trans. Faraday Soc.* **31**, 1892 (1935).
- ²E. H. Taylor and S. Datz, *J. Chem. Phys.* **23**, 1711 (1955).
- ³D. R. Herschbach, *Adv. Chem. Phys.* **10**, 319 (1966); J. L. Kinsey in *MTP International Review of Science*, edited by J. C. Polanyi (Butterworths, London, 1972), Vol. 9, p.173.
- ⁴F. E. Bartozcek, B. A. Blackwell, J. C. Polanyi, and J. J. Sloan, *J. Chem. Phys.* **74**, 3400 (1981).
- ⁵P. S. Weiss, J. M. Mestdagh, M. H. Covinsky, B. A. Balko, and Y. T. Lee, *Chem. Phys.* **126**, 93 (1988), and references 1–28 contained therein.
- ⁶D. Husain and P. Marshall, *Int. J. Chem. Kinet.* **18**, 83 (1986).
- ⁷J. M. C. Plane and E. Saltzman, *J. Chem. Phys.* **87**, 4606 (1987).
- ⁸D. Husain and Y. H. Lee, *Int. J. Chem. Kinet.* **20**, 223 (1988).
- ⁹M. Eliason and J. O. Hirschfelder, *J. Chem. Phys.* **30**, 1426 (1959).
- ¹⁰D. E. Jensen and G. A. Jones, *Combust. Flame* **32**, 1 (1978).
- ¹¹M. Shapiro and Y. Zeiri, *J. Chem. Phys.* **70**, 5263 (1979).
- ¹²M. M. Gallo and D. R. Yarkony, *J. Chem. Phys.* **86**, 4990 (1987).
- ¹³*JANAF Thermochemical Tables*, 3rd ed., edited by M. W. Chase, Jr., C. A. Davies, J. R. Downey, Jr., D. J. Frurip, R. A. McDonald, and A. N. Sverud, *J. Phys. Chem. Ref. Data* **14**, (1985).
- ¹⁴R. A. Goldberg and A. C. Aikin, *Science* **180**, 294 (1973).
- ¹⁵M. C. W. Sandford and A. J. Gibson, *J. Atmos. Terr. Phys.* **32**, 1423 (1970). J.-P. Jegou, M.-L. Chanin, G. Megie, and J. E. Blamont, *Geophys. Res. Lett.* **7**, 995 (1980).
- ¹⁶N. D. Sze, M. K. W. Ko, W. Swider, and E. Murad, *Geophys. Res. Lett.* **9**, 1187 (1982).
- ¹⁷L. Thomas, M. C. Isherwood, and M. R. Bowman, *J. Atmos. Terr. Phys.* **45**, 587 (1983).
- ¹⁸W. Swider, *J. Geophys. Res.* **92**, 5621 (1987).
- ¹⁹J. A. Silver, A. C. Stanton, M. S. Zahniser, and C. E. Kolb, *J. Chem. Phys.* **88**, 3123 (1986).
- ²⁰J. A. Silver and C. E. Kolb, *J. Phys. Chem.* **90**, 3267 (1986).
- ²¹J. A. Silver, D. R. Worsnop, A. Freedman, and C. E. Kolb, *J. Chem. Phys.* **84**, 4718 (1985).
- ²²E. Murad, W. Swider, and S.W. Benson, *Nature* **289**, 273 (1981); J.J. Lamb and S.W. Benson, *J. Geophys. Res.* **91**, 8683 (1986).
- ²³T. Shimazaki, *Minor Constituents in the Middle Atmosphere* (Reidel, Dordrecht, 1985).
- ²⁴C. Moller and M. S. Plesset, *Phys. Rev.* **46**, 618 (1934).
- ²⁵D. Husain, J. M. C. Plane, and Chen Cong Xiang, *J. Chem. Soc. Faraday Trans. 2*, **80**, 713 (1984).
- ²⁶J. M. C. Plane, *J. Phys. Chem.* **91**, 6552 (1987).
- ²⁷D. C. Brodhead, P. Davidovits, and S. A. Edelstein, *J. Chem. Phys.* **51**, 3601 (1969).
- ²⁸D. Husain and J. M. C. Plane, *J. Chem. Soc. Faraday Trans. 2* **78**, 163 (1982).
- ²⁹J. A. Silver, *J. Chem. Phys.* **81**, 5125 (1984).
- ³⁰A. A. Clifford, P. Gray, R. S. Mason, and J. I. Waddicor, *Proc. R. Soc. London Ser. A* **380**, 241 (1982).
- ³¹P. Palmieri, E. Garcia, and A. Lagana, *J. Chem. Phys.* **88**, 181 (1988).
- ³²GAUSSIAN 86, M. J. Frisch, J. S. Binkley, H. B. Schlegel, K. Raghavachari, C. F. Melius, R. L. Martin, J. J. P. Stewart, F. W. Bobrowicz, C. M. Rohlfing, L. R. Kahn, D. J. Defrees, R. Seeger, R. A. Whiteside, D. J. Fox, E. M. Fleuder, and J. A. Pople (Carnegie-Mellon Quantum Chemistry, Pittsburgh, 1984).
- ³³S. Carter and J. N. Murrell, *Mol. Phys.* **41**, 567 (1980).
- ³⁴I. W. M. Smith, *Kinetics and Dynamics of Elementary Gas Reactions* (Butterworths, London, 1980).
- ³⁵G. Schay, *Z. Phys. Chem. B* **11**, 291 (1930).
- ³⁶C. E. H. Bawn and A. G. Evans, *Trans. Faraday Soc.* **31**, 1392 (1935).
- ³⁷H. von Hartel, *Z. Phys. Chem. B* **11**, 315 (1930).
- ³⁸M. Polanyi, *Atomic Reactions* (Williams and Norgate, London, 1932).
- ³⁹A. Fontijn and R. Zellner, in *Reactions of Small Transient Species*, edited by A. Fontijn and M. A. A. Clyne, (Academic, London, 1983).
- ⁴⁰J. C. Slater and J. G. Kirkwood, *Phys. Rev.* **37**, 682 (1931).
- ⁴¹J. O. Hirschfelder, C. F. Curtiss, and R. B. Bird, *Molecular Theory of Gases and Liquids* (Wiley, New York, 1954).
- ⁴²D. R. Herschbach, in *Molecular Beams*, edited by J. Ross (Interscience, New York, 1966), p. 319.
- ⁴³M. F. Vernon, H. Schmidt, P. S. Weiss, M. H. Covinsky, and Y. T. Lee, *J. Chem. Phys.* **84**, 5580 (1986).
- ⁴⁴J. M. C. Plane and B. Rajasekhar, *J. Phys. Chem.* **93**, 3135 (1989).
- ⁴⁵C. H. Becker, P. Casavecchia, P. W. Tiedemann, J. J. Valentini, and Y. T. Lee, *J. Chem. Phys.* **73**, 2833 (1980).